ELSEVIER

Journal of Structural Geology 26 (2004) 1633–1645

JOURNAL OF STRUCTURAL GEOLOGY

www.elsevier.com/locate/jsg

Evidence of synextension tilting and doming during final exhumation from analysis of multistage faults (Queyras Schistes lustrés, Western Alps)

Pierre Tricart[a,*], Stéphane Schwartz[b], Christian Sue[c], Jean-Marc Lardeaux[d]

[a]*Labo. de Géodynamique des Chaînes Alpines, Observatoire des Sc. de l'Univers de Grenoble, Univ. J. Fourier, BP53, F-38041 Grenoble, Cedex 9, France*
[b]*BRGM, BP 6009, F-45060 Orléans, Cedex, France*
[c]*Institut de Géologie, Univ., CP 2, CH-2007 Neuchâtel, Switzerland*
[d]*Géosciences Azur, Institut de Géodynamique, 250 rue A. Einstein, Sophia-Antipolis, F-06560 Valbonne, France*

Received 31 March 2003; received in revised form 2 February 2004; accepted 4 February 2004

Available online 2 April 2004

Abstract

During the Neogene, the internal arc of the Western Alps underwent extension behind its inverted Paleogene frontal thrust while shortening affected the external arc. In the core of the internal arc, doming of eclogite-bearing gneissic nappes has formed the Dora–Maira massif. The blueschist-bearing Schistes lustrés of Queyras, which overlie the western flank of the Dora–Maira dome, allow observation of how the Neogene extension developed in ductile to brittle conditions. During the evolution from 'chocolate tablet' boudinage to cross-trend normal faulting, the extension kept a tendency to be multidirectional. The analysis of variably oriented fault families allows considering them as globally associated with the same long-lived tectonic regime. Focusing on faults bearing several generations of slickenlines and using an adapted right dihedra analysis, we propose that faulting accompanied the westwards tilting of the eastern Queyras structure. This tilting is consistent with the doming of the Dora–Maira massif, itself associated with tectonic denudation along its western flank. Therefore, two processes operated simultaneously during final exhumation: regional thinning through widespread multitrend normal faulting and more localised tectonic denudation and doming. Both are consistent with a Neogene regime dominated by vertical compression. The role of an ascending deep indenter below the internal arc remains to be documented.

Keywords: Ductile–brittle transition; Exhumation; Late orogenic extension; Right dihedra; Queyras Schistes lustrés; Western Alps

1. Introduction

Along the southern edge of Europe, the building of the Alps from the Late Cretaceous onwards, has resulted from subduction and subsequent collision processes in front of Adria indenter (see Schmid and Kissling, 2000 for review). During the Neogene, the external arc of the western Alps (Fig. 1) underwent increasing fold–thrust development while most of the internal arc underwent widespread extension (see Sue and Tricart, 2002 for review). In the core of the internal arc, the uplift of deeply exhumed continental basement nappes from below the oceanic Schistes lustrés complex, has formed the 'gneiss dome' structures of the Gran Paradiso and Dora–Maira, Internal Crystalline Massifs (Rolland et al., 2000; Agard et al., 2001; Schwartz et al., 2004; Tricart et al., 2004a). At the western foot of the (or Viso) ophiolitic slab that bounds the Dora–Maira massif to the west, the Piémont Schistes lustrés of Queyras (Figs. 2 and 3) have widely recorded the Neogene ductile to brittle extension. Thanks to a specific analysis using right dihedra, we show that normal faulting accompanied a regional-scale westward tilting in the western flank of the Dora–Maira dome that achieved this form. Therefore we confirm the close association of two processes active during the final exhumation of the Alpine innermost HP–LT metamorphic units: regional-scale extension and more localised doming and tectonic denudation.

2. Alpine tectonic context

The internal arc is derived from the Tethyan Ocean and its European margin (e.g. Tricart, 1984; Lemoine et al., 1986). The Briançonnais and Dora–Maira piles of nappes

* Corresponding author. Tel.: +33-4-76-51-40-72; fax +33-4-76-51-40-58.
E-mail address: ptricart@ujf-grenoble.fr (P. Tricart).

0191-8141/$ - see front matter © 2004 Elsevier Ltd. All rights reserved.
doi:10.1016/j.jsg.2004.02.002

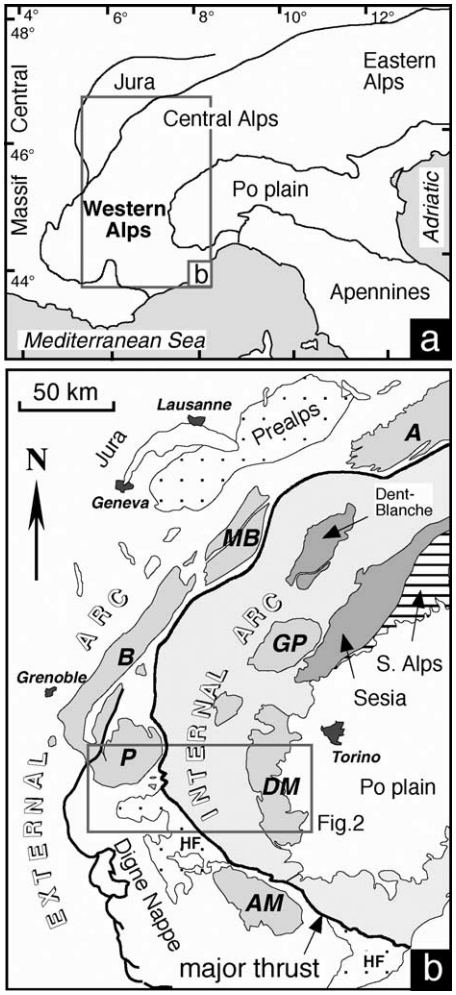

Fig. 1. Location maps. (a) Location of the Western Alps in the Alpine chain. (b) Simplified structural map of the Western Alps. The internal arc overrides the external arc along a major thrust mainly dated as Oligocene. Southeast of Pelvoux massif, it has been reactivated as a major extensional detachment (inverted Briançonnais frontal thrust; Sue and Tricart, 1999). East of it, most of the internal arc underwent extensional tectonics from the Miocene onwards (Sue and Tricart, 2002, 2003). The frame locates Fig. 2. External Crystalline Massifs: A, Aar; MB, Mont-Blanc; B, Belledonne; P, Pelvoux; AM, Argentera–Mercantour. Internal Crystalline Massifs: GP, Gran Paradiso; DM, Dora–Maira.

display essentially Tethyan sediments and pre-Alpine basement, respectively. Between them, an old accretionary wedge involves oceanic series and some remnants of the distal European margin (Schwartz, 2002; Tricart et al., 2004b). Metasediments dominate in the Queyras Schistes lustrés (Lemoine and Tricart, 1986), enclosing boudinaged ophiolitic bodies (Tricart and Lemoine, 1986). Thick ophiolitic nappes dominate in the Monviso massif (Lombardo et al., 1978; Philippot, 1988). Involved in younger polyphased isoclinal folds, the Queyras and Monviso piles of nappes presently dip westwards in conformity with the western flank of the Dora–Maira dome. Regionally, the HP–LT metamorphism grades up eastwards with jumps along tectonic contacts of various ages and nature (thrust versus extensional detachments): HP greenschists in Briançonnais; low grade (west) to high grade (east) blueschists in Queyras (Caby, 1996; Schwartz, 2002); various eclogites in Monviso (Lardeaux et al., 1987; Schwartz et al., 2000); imbricated eclogites and coesite bearing whiteschists (UHP) in Dora–Maira (Chopin et al., 1991).

This structure resulted from a long multistage history. The Late Cretaceous oceanic subduction was still active during the Early Eocene (Monviso: Duchêne et al., 1997), followed by the subduction of the lowermost margin, still active during the Late Eocene (Dora–Maira: Tilton et al., 1991; Duchêne et al., 1997). In this active margin context, the primitive Queyras accretionary wedge was already built during the Paleocene (Takeshita et al., 1994) and the central margin (Briançonnais zone) ended to be accreted to this wedge during the Late Eocene (Tricart, 1984). During the Oligocene transition to collision the Alpine internal arc was thrust onto the external arc and new folding–thrusting phases affected this internal arc. Through the classical backfolding and backthrusting movements, this explains the present-day Alpine fanning structure (Tricart, 1984). Before the end of the Oligocene, the thrust zone at the front of the internal arc (Briançonnais frontal thrust) began to be inverted as a major extensional detachment (Sue and Tricart, 1999; Tricart et al., 2001). To the east, extension developed in the internal arc during the Miocene, as a brittle extension in the Briançonnais nappes and as a ductile to brittle extension in the Piémont Schistes lustrés (Sue, 1998; Agard et al., 2001; Schwartz, 2002).

This 'late Alpine' extension accompanied the final exhumation of the HP–LT metamorphic units. In eastern Queyras and Monviso, Miocene fission track ages in Apatite and Zircon allowed estimation of a mean exhumation rate close to 0.4 mm/yr (Schwartz et al., 2004). Widespread extension in the internal arc continues presently, testified by seismotectonic (Sue et al., 1999; Delacou et al., 2004) and geodesy (Sue et al., 2000) surveys. In this paper, we focus on the brittle extensional structures affecting the Piémont Schistes lustrés in eastern Queyras and the surrounding French and Italian valleys.

3. Regional structure in Eastern Queyras

The eastern Queyras mountains display a huge mass of monotonous calcschists with an apparent monoclinal structure dipping towards the WSW (mean value close to 40°). Detailed mapping (Tricart et al., 2004b) showed that it represents a tilted pile of isoclinal folds, affecting early imbricated pellicular thrust sheets. Regional-scale isoclinal folds (F1), are associated with the primitive blueschist foliation. They have been refolded while the metamorphism evolved towards greenschist conditions. Folds of second generation (F2) are north-directed plurikilometric recumbent folds, contrasting with the south-verging third generation of folds (F3). The last folds (F4) are essentially

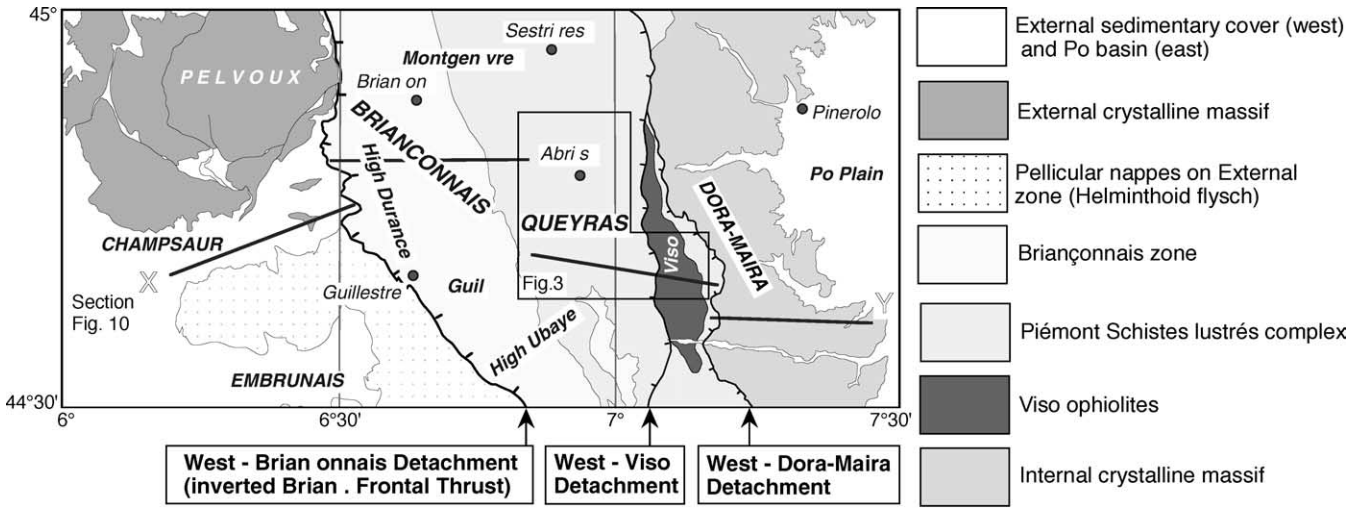

Fig. 2. Simplified structural map of the central part of the western Alpine arc. The west-dipping Viso and Dora–Maira detachments and the east-dipping west-Briançonnais detachment (inverted Briançonnais frontal thrust) represent major low-angle normal faults with conjugate movements. They contribute to the extension that developed in the internal arc during the Neogene and resulted in widespread normal faulting in the Briançonnais, Queyras and Monviso areas. The frame locates Fig. 3. X–Y, trace of the cross-section, Fig. 10.

minor asymmetrical folds with west-dipping axial surfaces. For a long time they have been attributed to the back movements i.e. to a last increase in the shortening–thickening of the regional structure, as in the Briançonnais zone (e.g. Tricart, 1975, 1984; Caron, 1977). This interpretation should be now restricted to the western Queyras Schistes lustrés, below the backthrust eastern Briançonnais zone. In eastern Queyras, they would rather represent drag folds resulting from bed-to-bed gliding within the foliation, in a top-down-to-the-west general shear.

This extensional shearing, driven by a faster uplift of more internal units (embryonic Dora–Maira massif?) has also been recognised just to the north (Agard et al., 2001); it corresponds to a thinning of the structure through tectonic denudation (see Tricart et al., 2004a for discussion). The onset of denudation tectonics was confirmed by the subsequent development of west-dipping extensional shear zones between eastern Queyras and Dora–Maira (west-Viso and west-Dora–Maira ductile normal faults in Fig. 2); they guide the extensional denudation of the Dora–Maira basement nappes below the Monviso ophiolites, themselves denuded below the eastern Queyras Schistes lustrés (Ballèvre et al., 1990; Black and Jayko, 1990).

Successive ductile deformations associated with shortening and subsequently with extension, accompanied the development of a strong omnipresent stretching lineation. Underlined by the last greenschist minerals, it lies within the plane of the regional foliation, corresponding to the primitive foliation variably transposed in younger cleavages; it may also lie within the late extensional shear zones; regionally it trends almost E–W, plunging westwards because of the general dip of the structure. While the syn-exhumation cooling of the Schistes lustrés continued, extension resulted in the boudinage of isolated beds, followed by a generalised normal faulting (see below) that would remain active today, down to 10–15 km depth (Sue and Tricart, 2002). We propose here that the westwards dip of the Schistes lustrés pile in eastern Queyras was mainly acquired during this normal faulting stage.

4. From boudinage to normal faulting in contrasted lithologies

Several sites recognized as demonstrative of the structural evolution that accompanied the regional-scale extension during final cooling are listed and located in Fig. 3. Calcschist-dominant metasediments enclosing thin competent beds of meta-arkose, in sites BA, VG and CV, allows observation of how boudinage predated normal faulting in contrasted lithologies. Similar behaviour may be observed where calcschists enclose beds of basalt-derived meta-arenites (the so-called Alpine ‘prasinites’) that may be up to several metres thick, e.g. in sites BB, 33 and CA. Other localities are demonstrative of normal faulting in a several hundred metres thick mass of metasediments with more homogeneous mechanical behaviour (sites LG, 7D, FP, CR and CL). Everywhere, including in the three preliminary sites located in the Monviso massif, observations are in accordance with the following reconstructed scenario.

Southwest of Pic d’Asti, in the highest part of Vallone del Giarus, isolated decimetric beds of meta-arkose lie within calcschists. They show how the extensional microstructures evolved while the regional structure entered into the brittle domain, during syn-exhumation cooling (Fig. 4). While the calcschists continued to flatten and stretch in a ductile way, enhancing their S + L structure associated with greenschist facies minerals, the enclosed meta-arkose beds underwent boudinage (detail in Fig. 4b). In apparent continuity, this

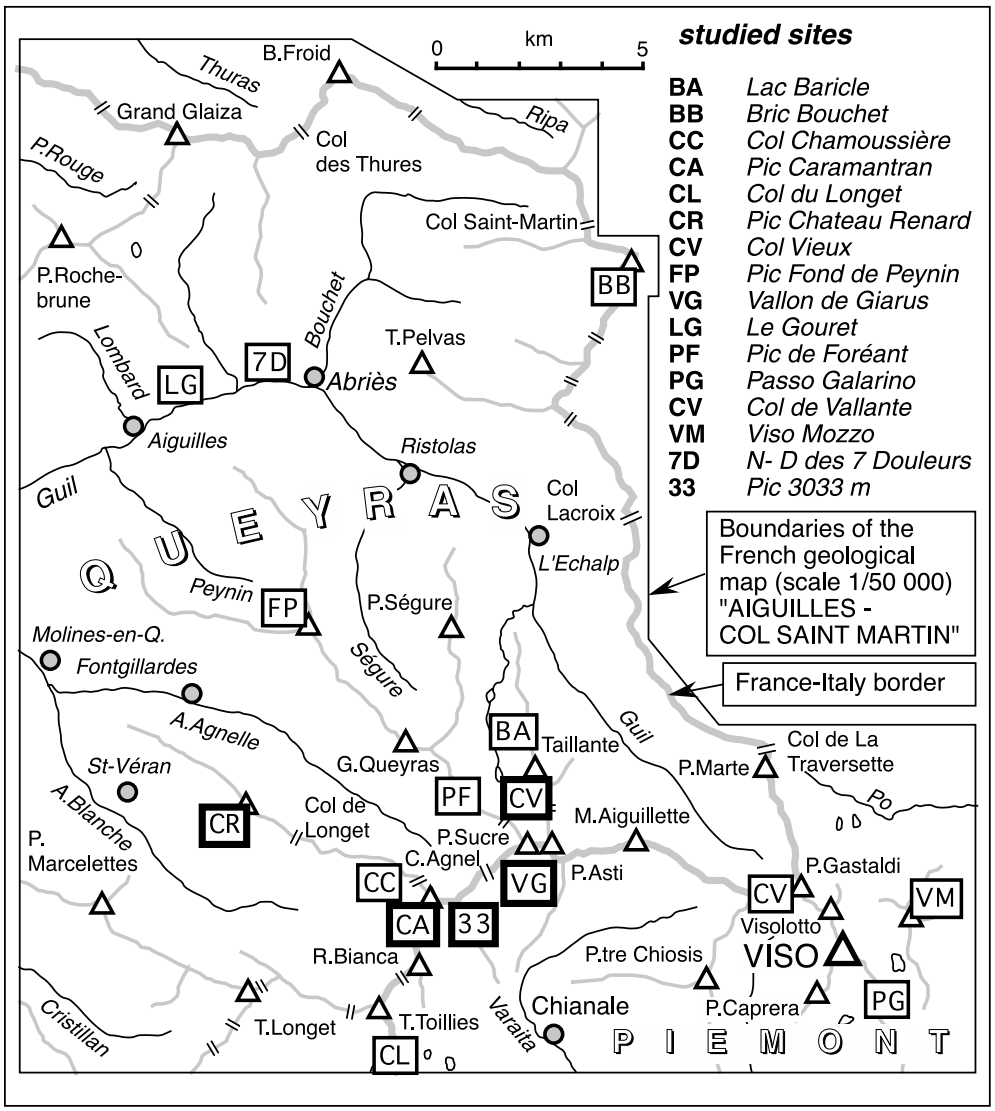

Fig. 3. Sketch-map of the Queyras–Viso area with location of the main analysed sites for the relations between brittle extension and westwards tilting of the regional structure. The French–Italian border follows the watershed between the Queyras and Piémont (Piedmont) regions. Boundaries of 'Aiguilles–Col Saint Martin' geological map according to Tricart et al. (2004b). Enhanced symbols for the sites illustrated here (CR, CA, 33, VG and CV).

boudinage evolved from unidirectional to multidirectional, testified by the development of two sets of sub-orthogonal quartz-filled veins (Fig. 4d). The resulting 'chocolate tablet' structure (Wegmann in Ramsay, 1967) constrains the stress–strain regime as a sub-horizontal almost radial spreading, accommodating a sub-vertical strong compression-shortening (Schwartz, 2002). Subsequently, normal faults developed in all lithologies, cutting through the whole bed pile. The persistence of a comparable stress regime is suggested by the high-angle pattern of the fault strikes (Fig. 4e). More in detail, the first faults to appear were micro-faults, often associated with important centimetric–decimetric drag folding (semi-ductile faults); they are systematically nucleated along the veins between the boudins (Fig. 4c).

Southwest of Pic d'Asti, as in all the other sites, small-scale normal faults appeared first, associated with drag-folds and/or en échelon arrays of tension gashes. These closely spaced early faults, which often evoke conjugate faults, display sub-orthogonal trends (Fig. 5). Greater scale isolated faults (e.g. Fig. 6b) only developed after, with increasing throw, characterizing an evolution from distributed towards more localised extension. Through this evolution,

Fig. 4. Faulted boudins in Vallone del Giarus site (VG in Fig. 3), at the southwestern foot of Pic d'Asti. (a) A contrasted lithology, corresponding to meta-arkoses (A) interbedded with Early Cretaceous calcschists (CS), has recorded the passing from ductile to brittle extension. The sedimentary pile is underlined by a west-dipping foliation containing a WSW–ENE stretching lineation that developed in greenschist metamorphic conditions when boudinage occurred within meta-arkoses; subsequently, micro-normal faulting affected the meta-arkoses and calcschists, as the whole pile became brittle. (b) Detail of a quartz-

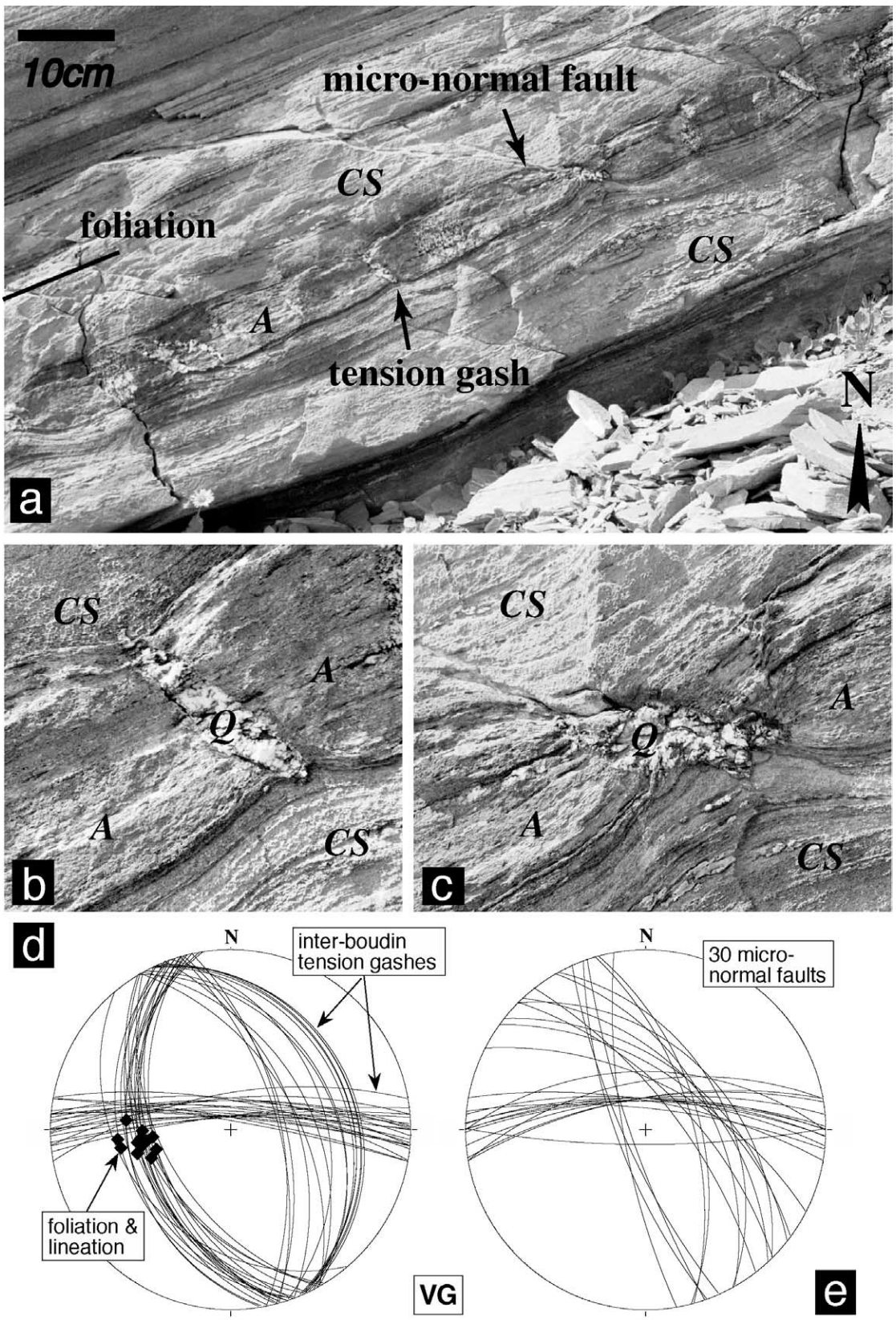

filled vein (Q), developed during the boudinage of meta-arkoses. (c) Detail of a comparable vein affected by micro-normal faulting and drag folding. Boudinage and faulting also occurred along a trend parallel to the outcrop. (d) and (e) Orientation of the illustrated small-scale structures (Wulff net, lower hemisphere, planes as great circles). Two suborthogonal sets of veins between boudins resulted in a chocolate tablet structure. The overprinting small normal faults display similar directions suggesting that radial extension during boudinage continued during faulting.

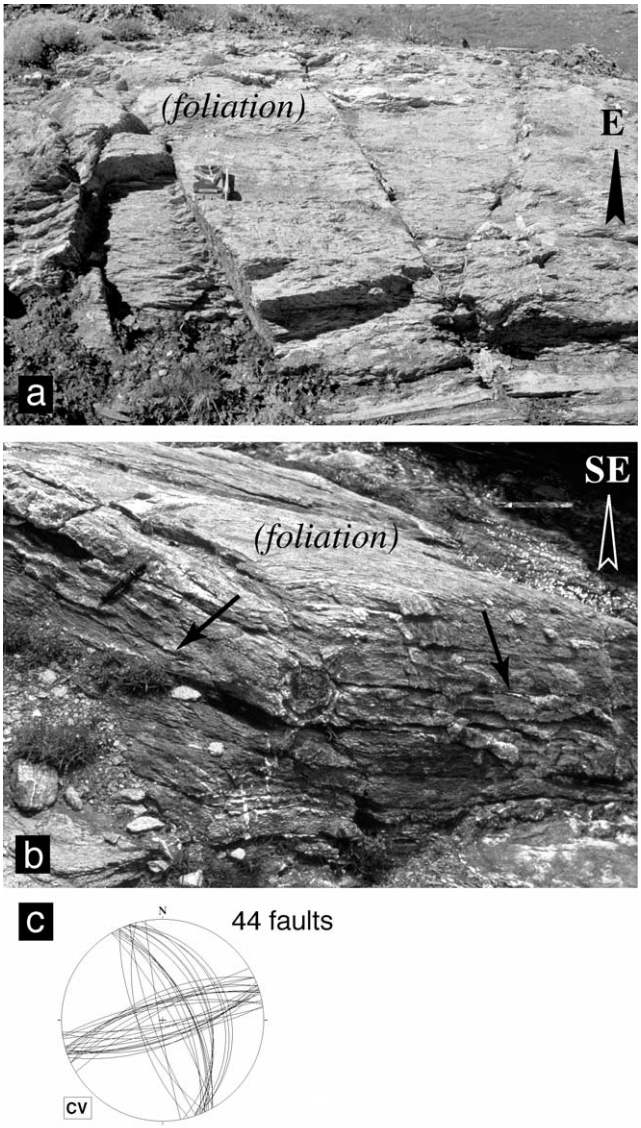

Fig. 5. Small-scale normal faults in thick meta-arkoses, around the point 2650 m, between Foréant lake and Col Vieux (site CV in Fig. 3). Foliation dips gently westwards. (a) E–W trending faults with drag folds indicating conjugate movements (compass for scale). (b) Two faults with orthogonal strikes (pen for scale), bearing oblique striae and quartz fibres (arrows). (c) Orientation of the fault planes (Wulff net, lower hemisphere, planes as great circles). Two sets dominate, with sub-orthogonal strikes; crosscutting relations indicate they are globally contemporaneous.

regional-scale faulting kept its multitrend nature (Fig. 6a), corresponding to an extension that tends to be radial. Variably pronounced from one site to another, more evident when considering the Queyras area as a whole, the multitrend nature of extension has been documented in most of the internal arc along the Queyras transect (Sue and Tricart, 2003).

Small, early brittle extensional structures have been systematically measured in eastern Queyras everywhere they could be clearly identified. On the assumption that pairs of conjugate normal faults were born with opposite dips of comparable value, and that the tension gashes were born along sub-vertical planes (Anderson, 1951), Schwartz (2002) estimated what was the original attitude of bedding when these structures appeared, i.e. when passing the ductile–brittle transition during syn-exhumation extension. Regionally, this original attitude was roughly sub-horizontal or gently dipping eastwards; it allowed the calculation of how much the beds have been tilted to reach their present-day west-dipping attitude: the proposed values for sites CV, VG, 33 and CA are 37°, 60°, 45° and 45° respectively. In the other site, they are dominantly in the 39–45° range.

5. Brittle deformation analysis

Structural analysis and mapping allowed the determination of the geometry of the fault network and the corresponding kinematics. In eastern Queyras, as in the whole Queyras–Briançonnais area, the most prominent fault sets cutting across the nappe pile trend N–S to NNW–SSE and E–W to NE–SW. Faults steepen in competent formations such as the marbles (Fig. 6c), the basalts and gabbros; they flatten, and may be listric, in the thick piles of calcschists (Fig. 6b). In all lithologies, drag folds, displaced beds, en échelon arrays of veins, sigmoidal veins, slickenfibres and other characteristic micro-structures on fault planes, clearly document the extensional nature of the late faulting. Locally, some very steeply dipping faults appear as reverse faults; in agreement with the following results (see Section 6 below) they can be interpreted as previous steep normal faults rotated with the faulted beds. In some areas also, the normal faults are overprinted by isolated major strike-slip faults, dominantly oriented N50–N80E with sinistral motion. The measurement sites have been chosen away from these late faults so that the smaller associated faults, locally abundant, are not concerned by the present study (see Sue and Tricart, 2003, for discussion).

Fault-slickenline populations have been sampled in the different sites localised in Fig. 3. In a limited rock volume, we tried to measure as many faults, with the largest scatter in attitudes, as possible. The dimensions of each measurement site are similar to a few hundred metres in diameter. Stereographic projections of original fault-stria data for the different sites confirm the multitrend nature of normal faulting, even if in a given site one trend family may dominate (Fig. 6a). For all the sites illustrated in this paper, as for the others concerned with this study, no data sorting was necessary and all the field measurements could be preserved when computing a single tectonic regime. The main stress axes were determined using the right dihedra method (Angelier and Mechler, 1977). Results confirm the sub-vertical direction for the compression (P) axis, in spite of the variations between lithologies (Fig. 7a). This characterizes an extensional tectonic regime. The tension (T) axis remains sub-horizontal or gently dipping but with poorly defined direction in all the investigated sites, possibly due to local permutation between T and intermediate (B)

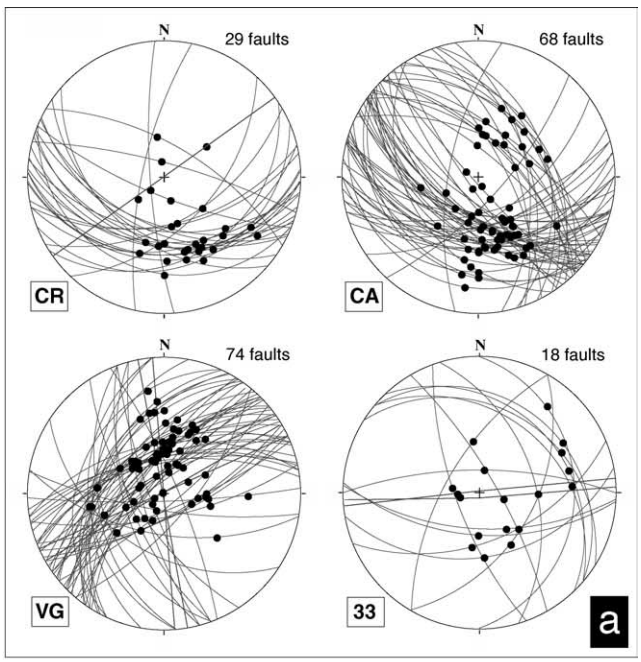

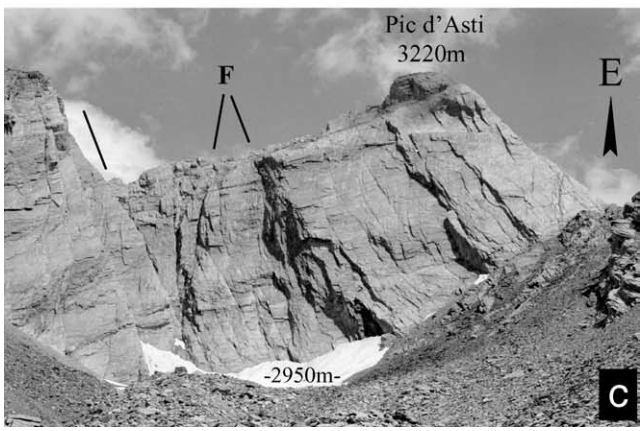

axes. This is consistent with the multitrend nature of the extension, already suggested from field observations (cross-cutting arrays of faults, chocolate tablet structures).

The same fault–slickenline populations were also analysed with the direct inversion method from Angelier (1990), using the TectonicVB software of Ortner et al. (2002). For the shape-ratio of the stress ellipsoid [$R = (\sigma_2 - \sigma_3)/(\sigma_2 - \sigma_3)$], it provided values lower than 0.5. For example, in the four illustrated sites (Figs. 6a and 7a), this value ranges between 0.25 (site VG) and 0.40 (site CA) confirming that the multitrend tendency for extension varies from one site to another.

An attempt to chronologically sort the faults, extending the pioneer work of Lazarre et al. (1994), aborted because the crosscut relationships between the different fault trend families appeared rapidly as non-compatible when considering wider areas of observation. Therefore we cannot confirm the chronology proposed by Agard et al. (2003) to the north of the present study area. On the contrary, we must conclude that all normal faults in all measurement sites, taken as a whole, allow the reconstruction of the same regional-scale and long lived tectonic regime. Doing so, our computed stress reduced tensors are comparable in all respects with those systematically computed by Sue and Tricart (2003) in the whole Queyras and adjacent areas.

6. Regional progressive tilting during normal faulting

The sub-vertical direction for the compression (P) axis determined from right dihedra analyses, characterizes an extensional tectonic regime (Table 1). Nevertheless, a closer look at the density stereoplots for the best P axis reveals that this axis varies in plunge towards the east (Fig. 7b). In addition, the amount of the plunge varies without corresponding variations in the amount of the westwards dip in the faulted beds. This suggests that successive normal faults develop in response to the same ongoing extensional tectonics, while the faulted structure was increasingly dipping westwards. A test of this hypothesis was possible using the fault planes bearing witness of more than one single strait motion.

Fig. 6. Normal faults affecting the whole visible structural pile. (a) Orientation of the fault–stria populations sampled in four sites (location in Fig. 3): Pic de Château-Renard (CR), Pic de Caramantran (CA), peak 3033 m high (33) and Vallone del Giarus (VG). Wulff net, lower hemisphere, fault planes as great circles and slickenlines as black dots. All faults are normal faults identified with drag folds, displaced beds and/or slickenfibres–growth sense. The measured faults display dominantly a single set of straight slickenlines. In the case of different successive movements, only the earliest slickenline has been plotted. (b) Faults in the foliated Late Cretaceous calcschists, eastern cliff of Pic de Château-Renard (2989 m). Cliff is 40 m high. F is a master listric fault, displaying curved slickenlines (fault plane with arrow in the foreground, detail in Fig. 8b). (c) Faults in west-dipping Tithonian marbles and Early Cretaceous calcschists, (site VG). Steep fault planes give the summits their pyramid-like relief.

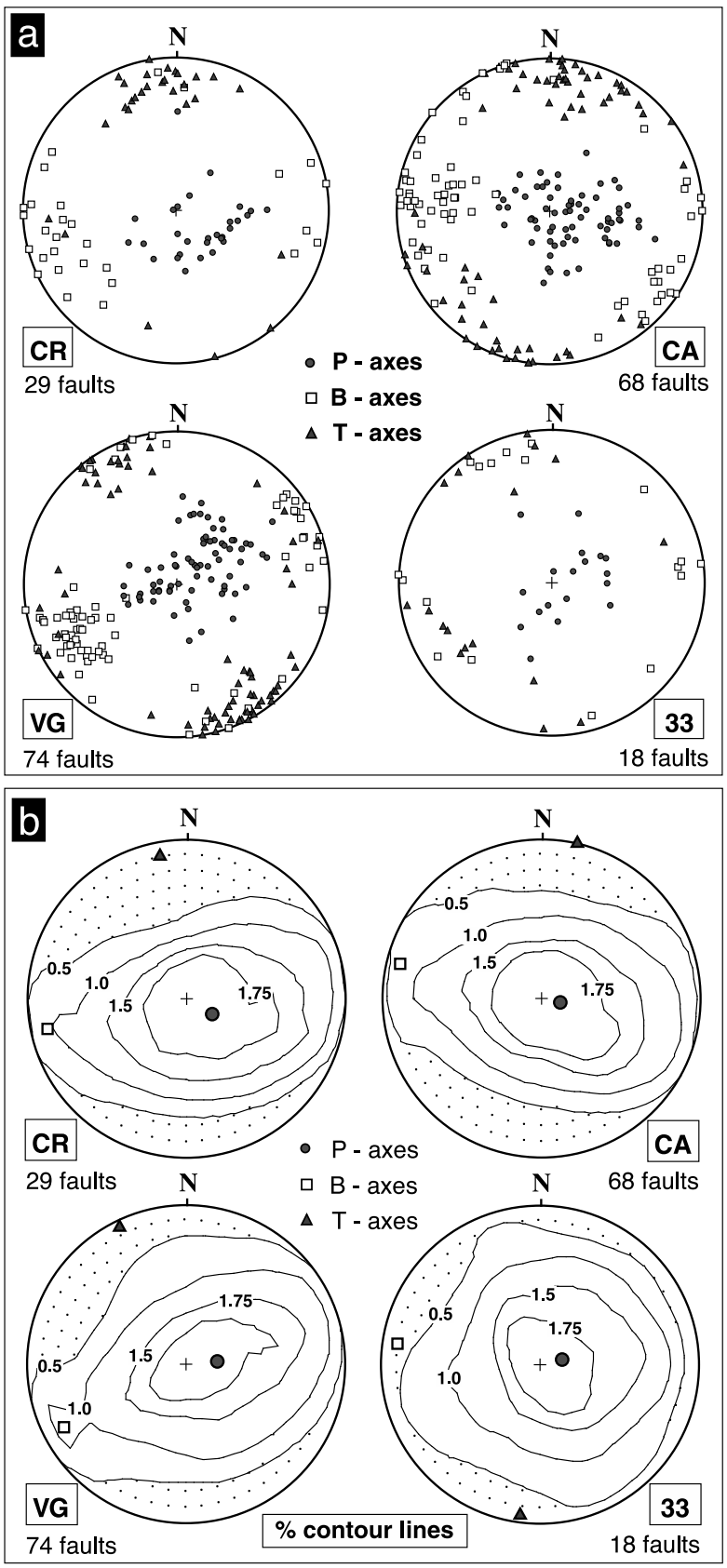

Fig. 7. Right dihedra analysis of the striated normal faults plotted in Fig. 6a, using TectonicVB software (Ortner et al., 2002; Schmidt net, lower hemisphere). (a) Computed *P* (compression), *T* (tension) and *B* (intermediate) axes from each striated fault. *P* axes lie preferentially near the plot centre (extensional regime) while *B* and *T* axes lie close to the peripheral great circle. *T* axes are mainly oriented close to N–S but also close to E–W. (b) Best axes from the whole fault populations and density contours for the compression (*P*) axis. The shift of the contour lines towards the right of the diagrams, in accordance with the eastwards steep plunge of the *P* axes, is explained by the westwards tilting of the structure during its faulting.

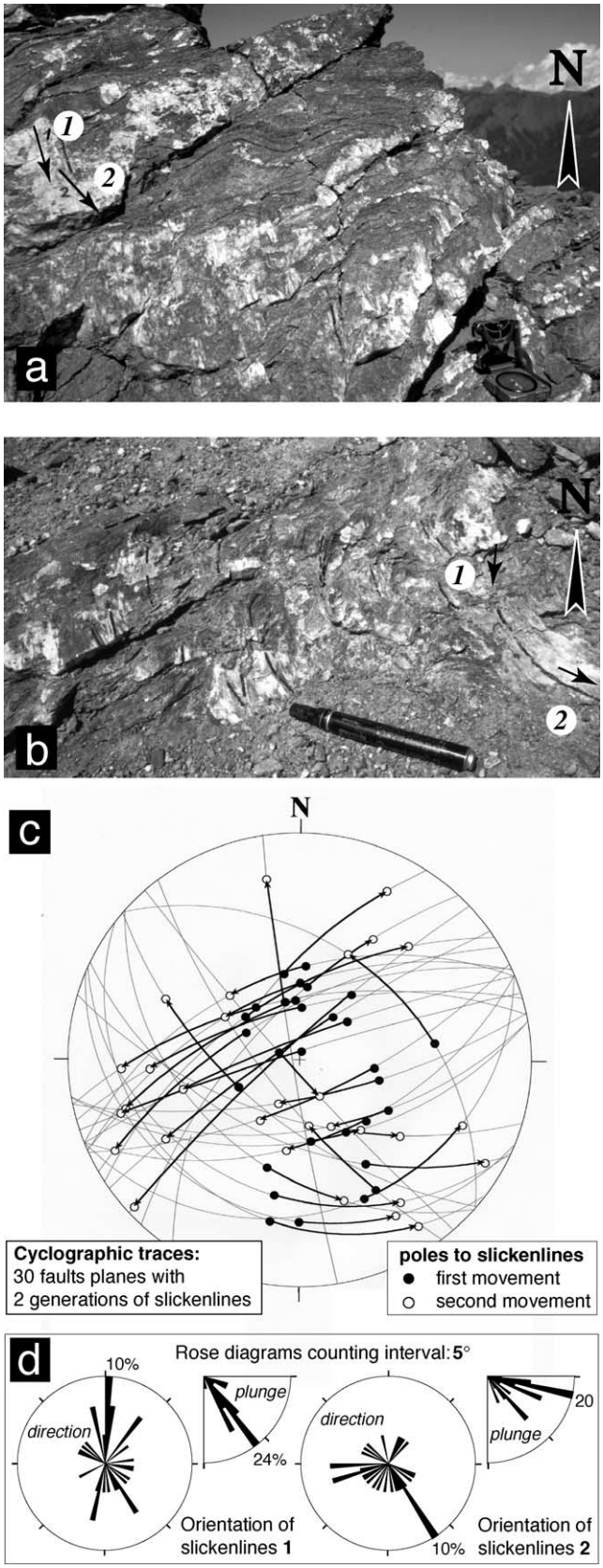

Fig. 8. Normal faults with different successive movements. (a) South-dipping fault plane in the Late Cretaceous calcschists of Pic de Château-Renard, 2989 m. Two generations of striae and calcite fibres correspond to a normal motion with a left-lateral component (1) that becomes more important during reactivation (2). (b) South-dipping fault plane in the same site with curved striae and calcite slickenfibres, indicating evolution through time from dip-slip normal faulting (1) to oblique slip with increasing sinistral strike-slip component (2). (c) Orientation of 30 normal faults selected in CR, CA, 33 and VG sites for their clear reactivation (slickenlines 2 overprinting slickenlines 1) or their progressive change in slip direction through time (curved slickenlines between direction 1 and direction 2). Each fault plane as great circle, bears two slickenlines as open and filled dots for movement 1 and 2, respectively. Along each fault plane trace, the curved arrow suggests the evolution of the slip direction from 1 to 2. Wulff net, lower hemisphere. (d) Rose diagrams for the slickenlines 1 and 2 plotted in (c). The strike-slip component of movement increased during reactivation.

In all sites, some multistage fault planes outcrop and special attention was paid to the chronology of the movements, using classical superimposition criteria. Many measurements were neglected due to non-perfectly established succession. Finally, we selected the measurements corresponding to two successive movements clearly distinguished, essentially thanks to distinct overprinted sets of slickenlines, in general calcite and/or quartz slickenfibres (Fig. 8a). The first slickenline family is interpreted as indicating the movement consecutive to the rupture (‘rupture stria’) providing information on the stress-state when the fault was propagating. The second slickenline family is interpreted as indicating evolved conditions during fault reactivation, when extension regionally increased (‘reactivation stria’). We also selected some nice fault planes bearing a single set of curved slickenfibres; only the oldest and youngest part of each slickenfibre were measured, the ‘intermediate’ slickenlines being ignored (Fig. 8b). The additional information here is that the movement was probably continuous between the first and the ‘second’ movement, through a rotation. The 30 selected faults are essentially located around the Pic de Château-Renard (site CR), Pointe des Fonzes (site PF) and along the watershed between the Brêche de Ruine to the north and the Col de Saint’Véran to the south (sites CV, VG, 33 and CA). These selected faults and their two generations of slickenlines display various orientations allowing the orientation of the main stress axes to be computed easily. All movements are extensional with a variable component of sinistral or dextral strike-slip. The stereoplot in Fig. 8c represents the 30 fault planes and, on each plane, the two generations of slickenlines measured on this plane. To facilitate their identification, a curved arrow follows each cyclographic trace joining the oldest slickenlines to the younger ones. In the case of curved slickenfibres, the arrow really describes the progressive change of the slipping direction through time. Globally, the mean pitch is greater for slickenlines 1 than for slickenlines 2 (Fig.8d).

These data were analysed with the right dihedra method (Fig. 9 and Table 1). The first analysis applies to the slickenlines 1. *T* axes are horizontal or gently plunging, with various directions. This characterizes a horizontal extension

Table 1
Orientation of best stress axes from right dihedra analysis: all faults in sites CR, CA, VG and 33 (stereoplots Fig. 7b) and 30 faults selected in these sites for the clear superimposition of two generations of slickenlines (stereoplots Fig. 9)

	P axis		*T* axis		*B* axis		Data
	Trend	Plunge	Trend	Plunge	Trend	Plunge	
Site CR	117	74	389	10	257	13	29
Site CA	103	79	012	00	282	11	68
Site VG	083	72	333	06	241	17	74
Site 33	077	78	202	07	294	10	18
Polystage faults:							
(all sites) striae 1	108	71	343	12	250	15	30
(all sites) striae 2	089	78	319	08	228	09	30

tending to be a multitrend extension (see Section 5 earlier). More importantly, many *P* axes plunge steeply to the east. We propose that starting from a vertical orientation corresponding to the faulting of sub-horizontal beds, they rotated variably with the beds, while normal faulting continued. This interpretation is consolidated when looking at the second stereoplot that applies to the slickenlines 2 worn by the same faults. The regime remains dominated by sub-horizontal extension and sub-vertical compression. The main difference is that the *P* axes are closer to the vertical; we propose that they were less rotated because the younger slickenlines have undergone a less important tilting. Comparing these stereoplots allows us to conclude that the beds were progressively rotated towards their present-day west-dipping attitude while normal faulting continued in response to the same vertical compression–horizontal extension tectonic regime. In this interpretation, in accordance with the classical faulting model of Anderson (1951), the continuation of normal faulting implies the appearance of new normal faults (with their slickenlines 1) and the reactivation (resulting in slickenlines 2) of older, more or less tilted faults (already bearing their slickenlines 1).

This result allows a better interpretation of the 'standard' fault-stria data collected in the different sites (Fig. 6a) and their diagrams resulting from right dihedra analysis (Fig. 7a). It appears that attention must be paid to the scattering of the computed *P* axes, between the vertical and an eastwards steeply plunging attitude. This scattering, more visible on adapted contour diagrams (Fig. 7b), would represent the specific signature of the westwards tilting of the structure during its faulting.

7. Discussion and conclusions

While the eastern Queyras structure evolved from ductile to brittle conditions during syn-exhumation final cooling, it remained submitted to an extensional tectonic regime, with some variations (variably pronounced multitrend character), but always dominated by a sub-vertical compression. During brittle extension, the coherence of our results from fault-stria analysis is consistent with the persistence of the same tectonic event, already suggested by direct field observations on the local and regional chronology of faults. This study shows that a westwards rotation of the beds accompanied the faulting. The coherence of results throughout all measurement sites, shows that this tilting affected the whole regional structure and was not restricted to isolated half-grabens, anyway not observed in the field. Preliminary observations suggest that this scenario would also be applied to the Monviso ophiolite pile (Schwartz, 2002).

To the North, Agard et al. (2003) proposed that an important rigid-body rotation of the whole Schistes lustrés structure occurred around a vertical axis while it underwent a pure unidirectional brittle extension. This rotation would explain the present-day multitrend character of the outcropping set of faults. Our analysis did not confirm this alternative interpretation. It implies that the rotation of the Briançonnais nappes recorded by paleomagnetism during the Neogene (Collombet et al., 2002) remains without an observed equivalent in the Queyras Schistes lustrés pile.

To the west, in western Queyras and more especially in Briançonnais (fault zone along the Durance valley; Fig. 10), the faulting regime acquired an increasing strike-slip nature through time before returning to the present-day seismotectonic extensional regime (see Sue and Tricart, 2003 for discussion). Poorly represented in eastern Queyras and Monviso, this evolution would post-date the scenario proposed here.

To the east, the final upwards bending of a pile of flat-lying crystalline basement nappes is at the origin of the present-day Dora–Maira massif with its N–S elongated (elliptic) antiformal structure. At the scale of the inner Alpine arc structure, readily visible along an E–W transect (Fig. 10), the west-dipping Schistes lustrés and ophiolites in the eastern Queyras and Monviso areas represent the western flank of the Dora–Maira dome. The final doming of the Dora–Maira nappes remains undated but it has to be connected with the movement of tilting reconstructed in this study. Doming and tilting accompanied a regional-scale brittle extension that was already active in the Miocene,

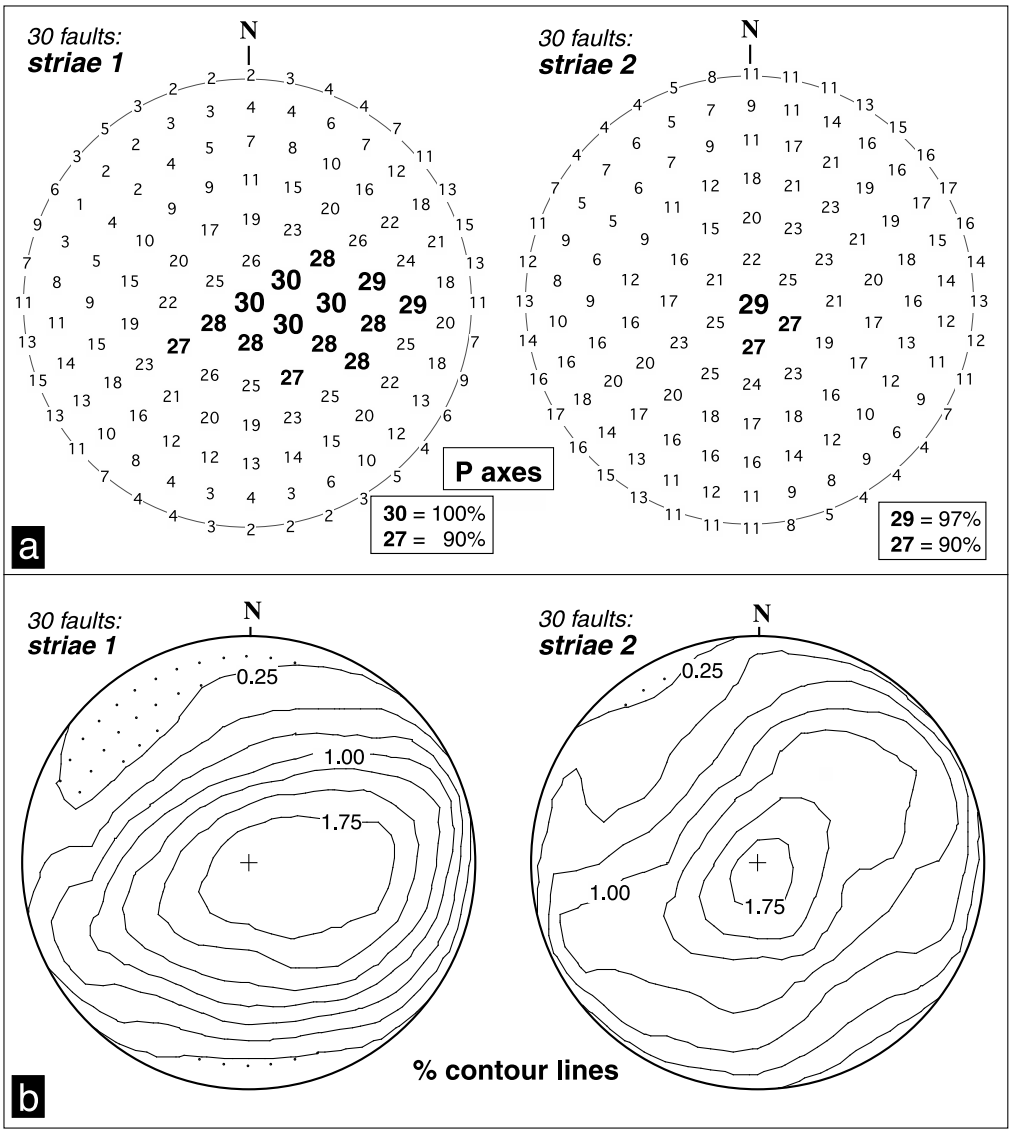

Fig. 9. Right dihedra analysis of the 30 selected faults plotted in Fig. 8c, computing separately slickenlines 1 and 2. All field measurements could be preserved, without any sorting. Schmidt net, lower hemisphere. (a) The plotted numbers indicate the number of faults with slickenlines that are consistent with the calculated compression axis (*P*). Computed *P* axes for the slickenlines 1: 100% vertical or steeply plunging eastwards; 90% are dominantly plunging eastwards. In response to vertical compression, faulting occurred during the westwards tilting of the beds, some at the beginning of the tilting and the others at a more advanced stage. Computed *P* axes for the slickenlines 2: 100% vertical and 90% sub-vertical. Fault reactivation or last movement (curved slickenfibres) along them, occurred while the beds were already close to the present-day west-dipping attitude, the main of the tilting being almost achieved. Fault software (Pêcher, unpublished). (b) Alternative representation with density contours for the best compression (*P*) axis: 0.25, 0.50, 0.75, 1.00, 1.25, 1.50 and 1.75%. Great circle distribution of *P* axes computed from rupture slickenlines ('striae 1') confirm they plunge variably eastwards. The cluster for *P* axes computed from reactivation slickenlines ('striae 2') correspond to a more vertical attitude. TectonicVB software (Ortner et al., 2002).

according to preliminary fission track ages in the Piémont Schistes lustrés (Schwartz et al., 2004).

Extensive exposure of previously deeply buried HP–LT metamorphic thrust sheets is the present-day characteristic of the innermost Alpine arc. Our analysis confirms that their final exhumation resulted from thinning and tectonic denudation driven by vertical compression and horizontal extension, in partly brittle (boudinage) to fully brittle conditions. In this context and at the scale of the internal arc, the final doming in the Dora–Maira massif and the induced regional tilting reconstructed here, can be seen as the expression of a faster uplift, i.e. a preferential exhumation, in the innermost part of the arc. This interpretation has to be consolidated by the calibration of the final P–T–t path of the Dora–Maira units. The Gran Paradiso massif that occupies a comparable position to the north must also share this evolution. Investigations continue to provide a better understanding of the role that could have been played here by a deep indenter such as the Ivrea slice of Adria mantle, the geometry of which was recently better-constrained (Fig. 10).

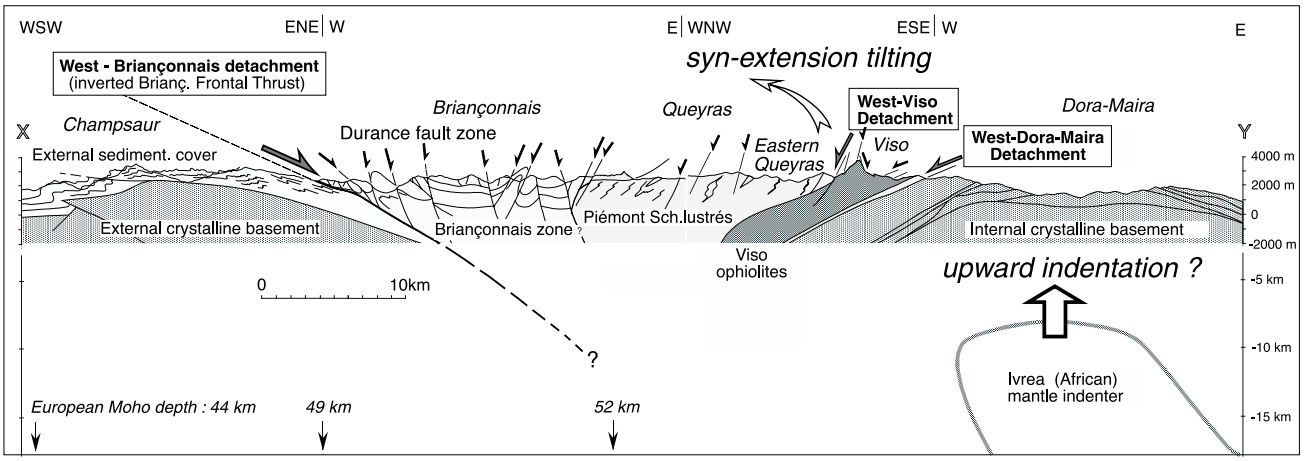

Fig. 10. General simplified cross-section of the internal arc, passing through the Queyras Schistes lustrés with prominent late extensional faults (location in Fig. 2). Geological structures from Tricart et al. (2004a), completed to the east (Dora–Maira) according to Michard et al. (1993) and Henry et al. (1993); depth of the European Moho from Thouvenot et al. (2004); Ivrea deep indenter from Paul et al. (2001). The Late Alpine evolution is enhanced. Two basement domes present similar dimensions but their tectonic meaning differ deeply. In the west the basement high below the Champsaur sandstones may be regarded as an embryonic External Crystalline Massif, uplift below the inverted major thrust at the front of the internal arc. In the east, the Dora–Maira Internal Crystalline Massif has been interpreted as a metamorphic core complex. Between them, the internal arc is cut up by numerous normal faults. The westwards tilting of the eastern Queyras Schistes lustrés and Monviso ophiolitic slab occurred during normal faulting, in response to the Dora–Maira final uplift and doming. The role of the Ivrea indenter remains hypothetical.

Acknowledgements

This work was supported by the French program Géo-France 3D and by the UMR 5025 (Unité Mixte de Recherche Joseph Fourier University and CNRS). Hugo Ortner adapted his 'TectonicVB' software to our specific needs. Arnaud Pêcher did the same with 'Fault' (right dihedra analysis of striated faults populations).

References

Agard, P., Jolivet, L., Goffé, B., 2001. Tectonometamorphic evolution of the Schistes lustrés complex: implications for the exhumation of the HP and UHP rocks in the western Alps. Bulletin de la Société Géologique de France 172, 617–636.

Agard, P., Fournier, M., Lacombe, O., 2003. Post-nappe brittle extension in the inner Western Alps (Schistes lustrés) following late ductile exhumation: a record of synextension block rotation? Terra Nova 15, 306–314.

Anderson, E.M., 1951. The Dynamics of Faulting, Oliver and Boyd, Edinburgh.

Angelier, J., 1990. Inversion of field data in fault tectonics to obtain the regional stress—a new rapid direct inversion method by analytical means. Geophysical Journal of the Interior 103, 363–376.

Angelier, J., Mechler, P., 1977. Sur une méthode graphique de recherche des contraintes principales également utilisable en tectonique et en séismologie: la méthode des dièdres droits. Bulletin de la Société Géologique de France 19(7), 1309–1318.

Ballèvre, M., Lagabrielle, Y., Merle, O., 1990. Tertiary ductile normal faulting as a consequence of lithospheric stacking in the western Alps. In: Roure, F., Heitzmann, P., Polino, R. (Eds.), Deep Structure of the Alps. Mémoire de la Société Géologique de France 156, pp. 227–236.

Black, M.C., Jayko, A., 1990. Uplift of very high pressure rocks in the western Alps: evidence for structural attenuation along low angle faults. In: Roure, F., Heitzmann, P., Polino, R. (Eds.), Deep Structure of the Alps. Mémoire de la Société Géologique de France 156, pp. 228–237.

Caby, R., 1996. Low-angle extrusion of high-pressure rocks and the balance between outward and inward displacements of Middle Penninic units in the western Alps. Eclogae Geologicae Helvetiae 89, 229–267.

Caron, J.M., 1977. Lithostratigraphie et tectonique des Schistes lustrés dans les Alpes cottiennes septentrionales et en Corse orientale. Sciences Géologiques Mémoire 48.

Chopin, C., Henry, C., Michard, A., 1991. Geology and petrology of the coesite bearing terrain, Dora–Maira massif, Western Alps. European Journal of Mineralogy 3, 263–291.

Collombet, M., Thomas, J.C., Chauvin, Y., Tricart, P., Bouillin, J.P., Gratier, J.P., 2002. Counterclockwise rotation of the western Alps since the Oligocene: new insights from paleomagnetic data. Tectonics 21, 278–293.

Delacou, B., Sue, C., Champagnac, J.D., Bburkhard, M., 2004. Present-day geodynamics in the bend of the western and central Alps as constrainedby earthquake analysis. Geophysical Journal International, in press.

Duchêne, S., Blichert-Toft, J., Luais, B., Télouk, P., Lardeaux, J.M., Albarède, F., 1997. The Lu–Hf dating of garnets and the ages of the Alpine high-pressure metamorphism. Nature 387, 586–589.

Henry, C., Michard, A., Chopin, C., 1993. Geometry and structural evolution of ultra-high-pressure and high-pressure rocks from the Dora–Maira Massif, Western Alps, Italy. Journal of Structural Geology 15, 965–981.

Lardeaux, J.-M., Nisio, P., Boudeulle, M., 1987. Deformational and metamorphic history at the Lago Superiore area of the Monviso ophiolitic complex (Italian Western Alps): a record of subduction–collision cycle? Ofioliti 12, 479–502.

Lazarre, J., Tricart, P., Villemin, T., 1994. L'extension cassante tardiorogénique dans les Schistes lustrés du Queyras (Alpes occidentales, France). Compte Rendus de l'Académie des Sciences Paris série II 319, 1415–1421.

Lemoine, M., Tricart, P., 1986. Les Schistes lustrés piémontais des Alpes occidentales: approche stratigraphique, structurale et sédimentologique. Eclogae Geologicae Helvetiae 79, 271–294.

Lemoine, M., Bas, T., Arnaud-Vanneau, A., Arnaud, A., Dumont, T., Gidon, M., Bourbon, M., Graciansky, P.-C.d., Rudkiewicz, J.-L., Mégard-Galli, J., Tricart, P., 1986. The continental margin of the Mesozoïc Tethys in the Western Alps. Marine and Petroleum Geology 3, 179–199.

Lombardo, B., Nervo, R., Compagnoni, R., Messiga, B., Kienast, J.R., Mevel, C., Fiora, L., Piccardo, G.B., Lanza, R., 1978. Osservazioni preliminari sulle ofioliti metamorfiche del Monviso (Alpi occidentali). Rendiconti Società Italiana Mineralogia Petrologia 34, 253–305.

Michard, A., Chopin, C., Henry, C., 1993. Compression versus extension in the exhumation of the Dora–Maira coesite-bearing unit, Western Alps, Italy. Tectonophysics 221, 173–193.

Ortner, H., Reiter, F., Acs, P., 2002. Easy handling of tectonic data: the programs TectonicVB for Mac and TectonicsFP for Windows (TM). Computers and Geosciences 28, 1193–1200.

Paul, A., Cattaneo, M., Thouvenot, F., Spallarossa, D., Bethoux, N., Frechet, J., 2001. A three-dimensional crustal velocity model of the southwestern Alps from local earthquake tomography. Journal of Geophysical Research Solid Earth 106(B9), 19367–19389.

Philippot, P., 1988. Déformation et éclogitisation progressives d'une croûte océanique subductée: le Monviso, Alpes occidentales. Contraintes cinématiques durant la collision alpine. Documents et travaux du Centre géologique et géophysique de Montpellier 19.

Ramsay, J.G., 1967. Folding and Fracturing of Rocks, McGraw-Hill, New York.

Rolland, Y., Lardeaux, J.-M., Guillot, S., Nicollet, C., 2000. Extension synconvergence, poinçonnement vertical et unités métamorphiques contrastées en bordure ouest du Grand Paradis (Alpes Franco-Italiennes). Geodinamica Acta 13, 133–148.

Schmid, S.M., Kissling, E., 2000. The arc of the western Alps in the light of geophysical data on deep crustal structure. Tectonics 19, 62–85.

Schwartz, S., 2002. La zone piémontaise des Alpes occidentales: un paléo-complexe de subduction. Arguments métamorphiques, géochronologiques et structuraux. Document du BRGM 302.

Schwartz, S., Lardeaux, J.M., Guillot, S., Tricart, P., 2000. Diversité du métamorphisme écologitique dans le massif ophiolitique du Monviso (Alpes occidentales, Italie). Geodynamica Acta 13, 169–188.

Schwartz, S., Lardeaux, J.M., Poupeau, G., Tricart, P., Labrin, E., 2004. New apatite and zircon fission-tracks data in the Piemontese zone of Western Alps: tectonic consequences. Tectonophysics, in press.

Sue, C., 1998. Dynamique actuelle et récente des Alpes occidentales internes—approche structurale et sismologique. Ph.D. thesis, University Joseph Fourier of Grenoble.

Sue, C., Tricart, P., 1999. Late Alpine brittle extension above the Frontal Pennine Thrust near Briançon, Western Alps. Eclogae Geologicae Helvetiae 92, 171–181.

Sue, C., Tricart, P., 2002. Widespread normal faulting in the Internal Western Alps: a new constraint on arc dynamics. Journal of the Geological Society 159, 61–70.

Sue, C., Tricart, P., 2003. Neogene to ongoing normal faulting in the inner western Alps. Tectonics, 22(5), 1050. DOI: 10.1029/2002TC001426.

Sue, C., Thouvenot, F., Fréchet, J., Tricart, P., 1999. Widespread extension in the core of the western Alps revealed by earthquake analysis. Journal of Geophysical Research 104(B11), 25611–25622.

Sue, C., Martinod, J., Tricart, P., Thouvenot, F., Gamond, J.F., Frechet, J., Marinier, D., Glot, J.P., Grasso, J.R., 2000. Active deformation in the inner western Alps inferred from comparison between 1972-classical and 1996-GPS geodetic surveys. Tectonophysics 320, 17–29.

Takeshita, H., Shimoya, H., Itaya, T., 1994. White mica K–Ar ages in blueschist–facies rocks from the Piemonte "calc-schists" of the western Italian Alps. The Island Arc 3, 151–162.

Thouvenot, F., Paul, A., Fréchet, J., Béthoux, N., Jenatton, L., Guiguet, R., 2004. 3-D constraints on the Moho in the south-western Alps: highlights of a new explosion-seismology experiment. Tectonophysics, in press.

Tilton, G.R., Schreyer, W., Schertl, H.P., 1991. Pb–Rb–Nd isotopic behaviour of deeply subducted crustal rocks from the Dora–Maira massif, western Alps, Italy—II: what is the age of the ultrahigh-pressure metamorphism? Contibution to Mineralogy and Petrology 108, 22–33.

Tricart, P., 1975. Les rétrocharriages dans les Alpes franco-italiennes: évolution des structures sur la transversale Embrunais—Queyras (Hautes-Alpes). Sciences Géologiques Bulletin 28, 239–259.

Tricart, P., 1984. From passive margin to continental collision: a tectonic scenario for the Western Alps. American Journal of Sciences 284, 97–120.

Tricart, P., Lemoine, M., 1986. From faulted blocks to megamullions and megaboudins: Tethyan heritage in the structure of the Western Alps. Tectonics 5, 95–118.

Tricart, P., Schwartz, S., Sue, C., Poupeau, G., Lardeaux, J.M., 2001. La dénudation tectonique de la zone ultradauphinoise et l'inversion du front briançonnais au sud-est du Pelvoux (Alpes occidentales): une dynamique miocène à actuelle. Bulletin de la Société Géologique de France 172, 49–58.

Tricart, P., Lardeaux, J.-M., Schwartz, S., Sue, C., 2004. Neogene to current extension in the Internal Western Alps: the overall situation along the Pelvoux–Viso transect. Tectonophysics, in press.

Tricart, P., Amaudric du Chaffaut, S., Ayoub, C., Ballèvre, M., Caby, R., Gout, C., Lagabrielle, Y., Leblanc, D., Le Mer, O.P.P., Saby, P., 2004. Carte géologique de la France, feuille 848 Aiguilles-Col Saint Martin. Bureau de Recherches Géologiques et Minières, scale 1:50,000.